

ANALYSIS OF AN ELECTROFORCED SEDIMENTATION OF HIGHLY CONCENTRATED CLAY SLURRY IN CONSOLIDATION REGION

Won Deok Yi[†] and Masashi Iwata*

Kum Yang Engineering Co., Ltd. (#301 Dong San Bldg.), 77-3, 4ka, Jung Ang-dong, Jung-ku, Pusan, Korea

*Department of Industrial Chemistry, Suzuka National College of Technology, Shiroko-Cho, 512-02, Suzuka, Japan

(Received 9 May 1995 • accepted 28 July 1995)

Abstract—A gravitational settling rate of highly concentrated slurry in which thickening proceeds due to consolidation mechanism is greatly enhanced by applying a D. C. electric field. Consolidation starts from the bottom of sediment and propagates upwards, but an abnormally strong consolidation also takes place in an upper portion of the sediment. The basic differential equation for such electroforced sedimentation is derived by use of Kobayashi's equation which describes a flow in a porous material under an electric field. The relation among local hydraulic excess pressure, solid compressive pressure and gravitational force on solid particles is also obtained. Based on the theory, the larger the porosity of sediment, the greater the flow rate of electroosmosis; the electroosmotic flow at the settling surface is accordingly the largest among those at any layers in the sediment. An abnormal compaction of the layer near the settling surface is consequently due to the difference between flow rates at the surface and any layer under the surface. The theoretical change of porosity distribution and sediment height with time of Mitsukuri-Gairome clay compares favorably with experimental observations.

Key words: Solid Liquid Separation, Sedimentation, Consolidation, Electroosmosis, Highly Concentrated Slurry

INTRODUCTION

Sedimentation of highly concentrated slurries in which solid particles contact each other is controlled by the consolidation mechanism, and usually proceeds at a very low settling rate. Although the improvement of settling rate of dilute suspensions (e.g. by use of flocculant) has received much attention, relatively little has been focused on the enhancement of settling rate of highly concentrated suspension. Shirato et al. [Shirato et al., 1979] has reported that the application of D.C. electric field is remarkably effective to increase the settling velocity of highly concentrated material. This is mainly due to an electroosmotic flow which results from the presence of an electrical double layer along a solid-liquid interface. The application of the electric field causes the ions in the double layer to move towards one electrode or the other. Since the ions are predominantly of one sign their motion gives rise to a body force on the liquid in the double layer, and it is this body force which sets the liquid in motion.

Consolidation proceeds from the bottom of the settling sediment, but an abnormally strong consolidation also takes place in an upper portion of the sediment. Shirato et al. discussed the mechanism of electroforced sedimentation, but failed to explain the consolidation in the upper portion of the sediment.

In the previous paper [Iwata et al., 1991], an analytical method for electroosmotic dewatering of compressible materials was presented, in which the tortuosity of a flow path and the effect of the hydraulic pressure profile in the materials were considered. Here we develop a conceptually similar model for consolidation under electroforced sedimentation, which successfully correlates our data.

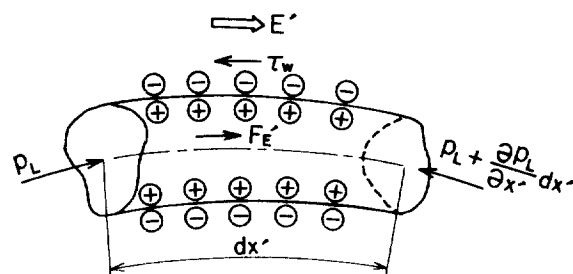


Fig. 1. Forces acting over a liquid in a tortuous flow path.

THEORY

1. The Apparent Velocity, of Liquid through Sediment

In the development of theoretical model for flow under electroforced sedimentation, the flow paths in a settling sediment are represented by non-circular ducts of arbitrary geometry, as shown in Fig. 1. The force balance among electrokinetic force F'_E per unit inner surface area, hydraulic excess pressure p_L and shear stress τ_w acting on the liquid in the duct of infinitesimal length is given by

$$\begin{aligned} & (\text{wetted cross-sectional area}) \left\{ p_L - \left(p_L + \frac{\partial p_L}{\partial x'} dx' \right) \right\} \\ & = (\text{wetted perimeter}) dx' (\tau_w - F'_E) \end{aligned} \quad (1)$$

By use of the extended Rabinowitsch-Mooney equation [Kozicki et al., 1966], τ_w in Eq. (1) is represented by a mean velocity of liquid U_b ,

$$\tau_w = \frac{4K_0\mu}{D_r} U_b \quad (2)$$

where K_0 is the geometric constant [Kozicki et al., 1967]; μ , the

[†]To whom all correspondences should be addressed.

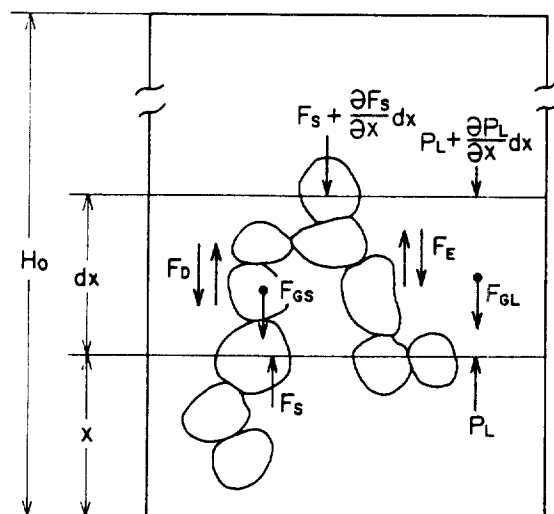


Fig. 2. Forces acting over the slice dx of the sediment.

viscosity of the fluid; D , the equivalent diameter of the flow path. F'_E is given by

$$F'_E = \frac{\xi DE'}{\delta} \quad (3)$$

where ξ is the zeta-potential of the electric double layer; D , the dielectric constant of fluid; E' , the electric field intensity along the real flow path; and δ , the double layer thickness. Combining these equations yields Kobayashi's equation which gives the apparent velocity q of liquid through the sediment [Iwata et al., 1991; Kobayashi et al., 1979].

$$q = \frac{1}{\mu\alpha\rho_s} \left(\frac{\sigma_s i \rho_E}{\varepsilon} - \frac{\partial p_L}{\partial \omega} \right) \quad (4)$$

The first term of the right-hand side of Eq. (4) represents an electroosmotic flow, while the second term shows a pressure flow; both being considered the tortuosity of the flow path. Here α is the specific hydrodynamic resistance of sediment; σ_s , the effective charge on solid surface per unit volume of solids; i , the electric current density; ρ_E , the specific electric resistance of sediment; and ε , the local porosity. ω in Eq. (4) is the moving material coordinates [Shirato et al., 1967]; i.e. the volume of solids per unit cross-sectional area measured from the bottom of sediment.

2. Relation between Hydraulic Excess Pressure and Solid Compressive Pressure

The local porosity ε of the sediment depends upon the local solid compressive pressure p_s . The relation between p_L and p_s is accordingly essential to obtain a theoretical structure of sediment. Forces acting over the slice dx of the sediment are shown in Fig. 2. F_D and F_E in the figure respectively denote the viscous drag and the electrokinetic force acting on unit surface area of solid particles. F_s is the solid compressive force. $F_{GS}(=\rho_s g)$ and $F_{GL}(=\rho g)$ are the gravitational force on solid and liquid, respectively, per unit volume. The balance of force acting on the solid and the liquid respectively over the slice dx can be represented by the following equations.

$$\begin{aligned} -A \frac{\partial(1-\varepsilon)p_L}{\partial x} dx - \frac{\partial F_s}{\partial x} dx + Adx(1-\varepsilon)S_0 F_D \\ - Adx(1-\varepsilon)S_0 F_E - Adx(1-\varepsilon)\rho_s g = 0 \end{aligned} \quad (5)$$

$$\begin{aligned} -A \frac{\partial \varepsilon p_L}{\partial x} dx - Adx(1-\varepsilon)S_0 F_D + Adx(1-\varepsilon)S_0 F_E \\ - Adx\varepsilon\rho g = 0 \end{aligned} \quad (6)$$

where A denotes the cross-sectional area of a settling tube; p_L , the hydraulic pressure [i.e. $P_L = p_L + \rho g(H_0 - x)$]; and S_0 , the volumetric specific surface. Combining Eq. (5) with Eq. (6) and defining the solid compressive pressure by $p_s = F_s/A$ yields

$$\frac{\partial p_L}{\partial x} + \frac{\partial p_s}{\partial x} = -(1-\varepsilon)(\rho_s - \rho)g \quad (7)$$

or on the material coordinate

$$\frac{\partial p_L}{\partial \omega} + \frac{\partial p_s}{\partial \omega} = -(\rho_s - \rho)g \quad (8)$$

It should be noted that the surface forces F_E and F_D do not appear in Eqs. (7) and (8), i.e. the relation among p_L , p_s and the gravitational force is the same as in gravitational sedimentation due to consolidation mechanism [Shirato et al., 1970]. Substitution of Eq. (8) into Eq. (4) yields

$$q = \frac{1}{\mu\alpha\rho_s} \left\{ \frac{\sigma_s i \rho_E}{\varepsilon} + \frac{\partial p_s}{\partial \omega} + (\rho_s - \rho)g \right\} \quad (9)$$

3. Basic Differential Equation of Electroforced Sedimentation

The mass balance of liquid with respect to the volume element $d\omega$ gives the continuity equation:

$$\frac{\partial e}{\partial \theta} = -\frac{\partial q}{\partial \omega} \quad (10)$$

where e denotes the local void ratio defined by $e = \varepsilon/(1-\varepsilon)$. Substitution of Eq. (9) into Eq. (10) yields the basic differential equation which controls the progress of electroforced sedimentation.

$$\frac{\partial e}{\partial \theta} = -\frac{\partial}{\partial \omega} \left[\frac{1}{\mu\alpha\rho_s} \left\{ \frac{\sigma_s i \rho_E}{\varepsilon} + \frac{\partial p_s}{\partial \omega} + (\rho_s - \rho)g \right\} \right] \quad (11)$$

Eq. (11) is reduced to the equation for gravitational settling due to consolidation [Shirato et al., 1970] if $i=0$. The initial and boundary conditions for Eq. (11) can be described as

$$p_s = p_0 \text{ at } \theta = 0 \quad (12)$$

$$p_s = p_0 \text{ at } \omega = \omega_0 \text{ (surface of sediment)} \quad (13)$$

$$\frac{\partial p_s}{\partial \omega} = -\frac{\sigma_s i \rho_E}{\varepsilon} - (\rho_s - \rho)g \text{ at } \omega = 0 \text{ (bottom)} \quad (14)$$

where p_0 denotes the value of p_s corresponding to the initial concentration of suspension and can be determined from the compression data described below. Eq. (14) is equivalent to the impermeable bottom condition ($q=0$). Strictly, Eq. (13) should be applied at $\omega_0^* = \omega_0 - p_0/(\rho_s - \rho)g$, because only below the layer $\omega = \omega_0^*$ will the net weight of solid particles $(\rho_s - \rho)(\omega_0 - \omega)g$ become larger than the initial strength p_0 of the suspension network. However, since p_0 is usually very small, we may use Eqs. (12)-(14) as initial and boundary conditions for simplicity of calculations.

EXPERIMENTAL

1. Experimental Apparatus and Procedure

The apparatus used for the sedimentation experiments is shown in Fig. 3. It consisted of a plexiglass cylinder with inside diameter of 5 or 10 cm and a pair of top and bottom brass disk electrodes; the top electrode disk is perforated so that the small

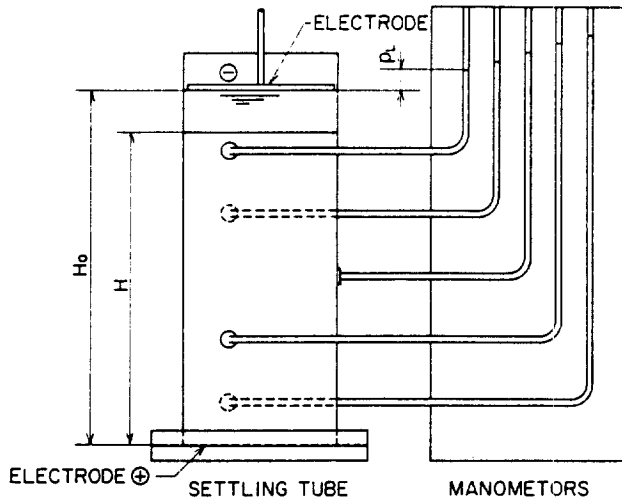


Fig. 3. Experimental settling tube.

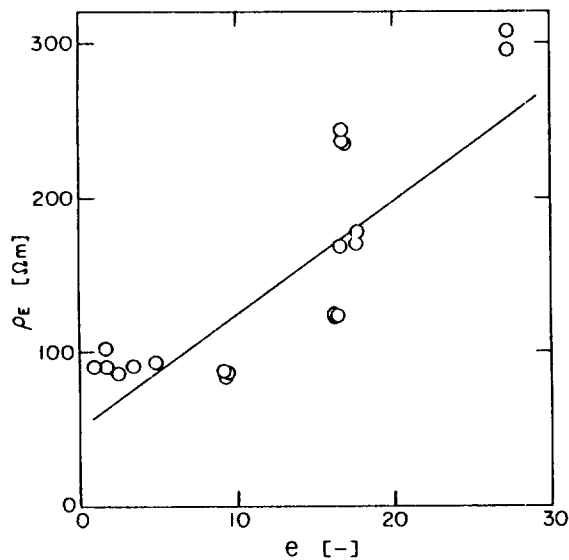


Fig. 4. Specific electric resistance ρ_E of Mitsukuri-Gairome Clay slurry.

amount of gas created by electrolysis can be removed. As the experimental material, Mitsukuri-Gairome Clay was used. The clay-deionized water suspensions were prepared in high concentration region where the settling proceeds under consolidation mechanism; based on a work of Shirato et al. [Shirato et al., 1979]. Mitsukuri-Gairome Clay suspension settles due to consolidation mechanism when $\epsilon < 0.966$.

The height of the settling sediment H was measured with the lapse of time θ . The hydraulic excess pressure p_E distributions were obtained by use of capillary manometers shown in Fig. 3. Porosity distributions in sediments were measured by weighing; i.e. at a settling time θ , supernatant was siphoned out and the settling sediment was sucked into several pipettes in the regular sequence of the depth of sediment, followed by direct weighing of each sample.

2. Physical Properties of Mitsukuri-Gairome Clay

2-1. Compression-permeability Characteristics

Relation among α , ϵ and p_s were determined by the sedimenta-

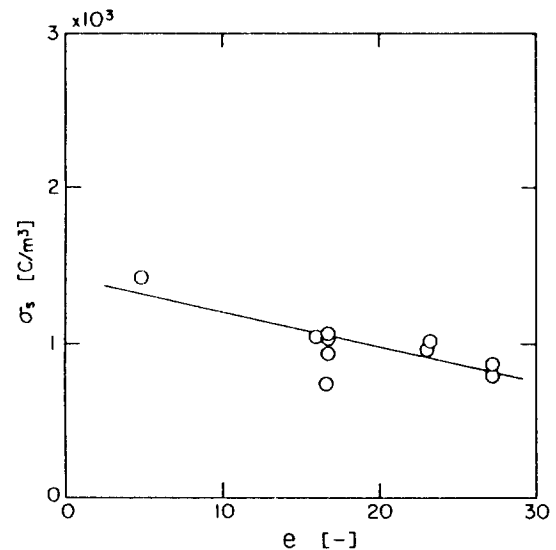


Fig. 5. Effective electric charge density σ_s of Mitsukuri-Gairome Clay.

tion test under the gravity [Shirato et al., 1970; Shirato et al., 1979].

They are correlated as

$$\alpha = 1.5 \times 10^{10} \exp\{39.8(0.966 - \epsilon)\} \quad (\epsilon < 0.966) \quad (15)$$

$$\epsilon = 1 - 0.0498 p_s^{0.101} \quad (\epsilon = 0.905 - 0.919) \quad (16)$$

2-2. Specific Electric Resistance ρ_E

Electric resistance of suspension with a uniform porosity was determined from initial electric current and applied voltage. ρ_E increases with increasing e as shown in Fig. 4. In the theoretical calculation, we use the solid line in Fig. 4 as approximate relation between specific electric resistance and void ratio.

2-3. Effective Electric Charge Density on Solid Surface σ_s

Solid compressive pressure p_s can be assumed constant throughout the height at the beginning of electroforced sedimentation of a uniform suspension. σ_s can be accordingly determined from the initial settling velocity v_0 on referring to Eq. (9), i.e.

$$\sigma_s = \frac{\{v_0 \mu \alpha p_s - (\rho_s - \rho)g\} \epsilon}{i \rho_E} \quad (17)$$

σ_s can be correlated with e as shown in Fig. 5.

RESULTS AND DISCUSSION

Figure 6 shows change of sediment height H with time under electroforced sedimentation. It can be seen from the figure that settling velocities increase remarkably with increasing field intensity E . The enormous enhancement of settling velocity suggests the possible application of electroforced sedimentation to separations of solid-liquid mixtures of extremely low settling velocities. Porosity distributions in the sediments at $\theta = 180$ min are illustrated in Fig. 7 for various E values. At this moment, except for the case of $E = 31.1$ V/m, remarkable compactions are observed not only in the bottom layers but also in the upper portions of the settling sediments. It should be noted, however, that at $\theta = 360$ min the upper compaction was observed even in the case of $E = 31.1$ V/m.

Figure 8 shows a typical result of a measurement of hydraulic

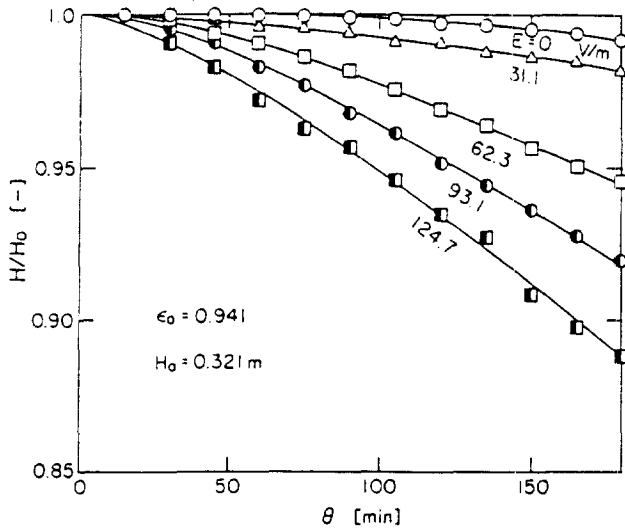


Fig. 6. Effect of electric field intensity E on settling rate.

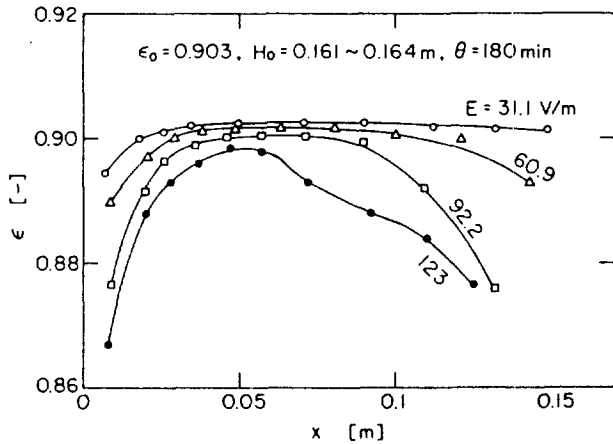


Fig. 7. Effect of electric field intensity E on porosity distribution.

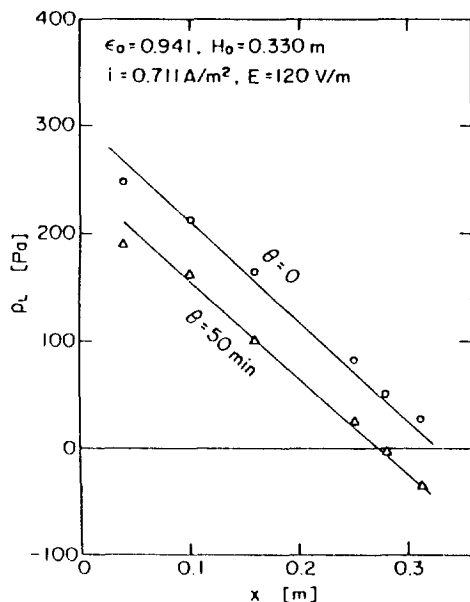


Fig. 8. Hydraulic excess pressure distribution through a settling sediment.

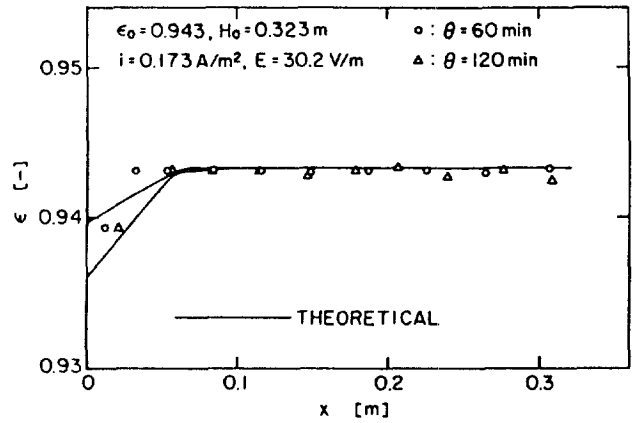


Fig. 9. Comparison of theory and experiment under normal consolidation.

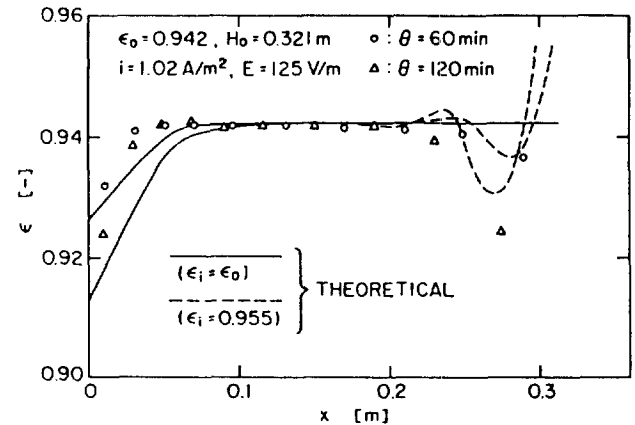


Fig. 10. Comparison of theory and experiment accompanying consolidation of upper layer of sediment.

excess pressure in the sediment. At the beginning of sedimentation, the gravitational force on solid particles above any layer of the sediment should be entirely sustained by the hydraulic excess pressure p_L at the layer. As consolidation proceeds, p_L is replaced by the solid compressive pressure p_s in accord with Eq. (8). It is interesting to note that at $\theta=50$ min negative values of p_L appear in the upper portions of the sediment. This means that the pressure flow is locally directed from the sediment surface to the bottom. It suggests that the electroosmotic flow at the surface may be extremely large and the pressure flow in the opposite direction may compensate a part of it.

In Figs. 9 and 10, calculated values from Eq. (11) are compared with experimental ones. Solid lines in the figures represent theoretical ϵ -distributions using the initial and boundary conditions Eqs. (12)-(14). The agreement between theory and experiment is satisfactory near the bottom of a settling tube, while in upper portions of the sediments the theoretical value is held constant because of Eq. (13). Figure 11 shows a typical photograph near the settling surface under an electric field. Cloudy liquid layer suggests that electroosmotic flow disturbs the arrangement of solid particles in the surface layer. On the other hand, such cloudy layer does not appear when $E=0$. Since the first term in the right-hand side of Eq. (9) is much greater than the others in upper portion of the sediment, the electroosmotic flow

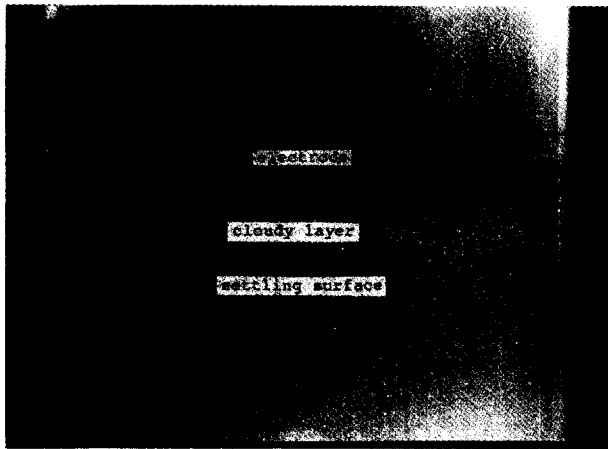


Fig. 11. Typical photograph of settling surface under an electric field ($\epsilon_0=0.942$, $E=125$ V/m).

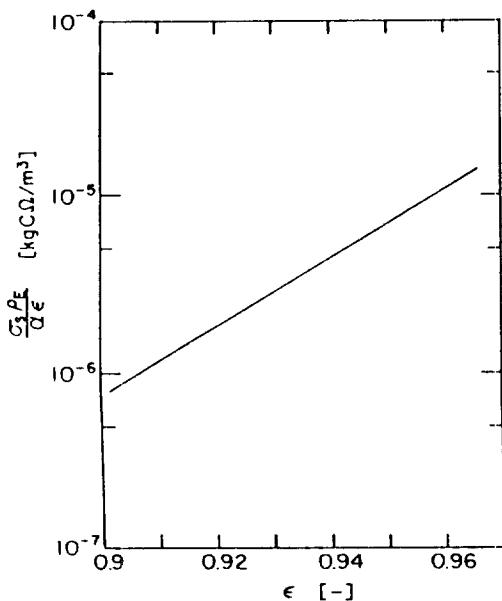


Fig. 12. Factor which determines the magnitude of electroosmotic flow.

may cause such disturbance of the sediment surface. The value of $\sigma_r\rho_E/\alpha\epsilon$ in Eq. (9), which determines the magnitude of electroosmotic flow, increases with increasing porosity ϵ as shown in Fig. 12. The porosity at the sediment surface becomes greater than its initial value, since an electroosmotic flow disturbs the layer as mentioned above; the electroosmotic flow rate at the surface layer is consequently greater than that at any other layer below the surface. The porosity in the portion between the surface and any other layers should accordingly decrease. The broken lines in Fig. 10 are such theoretical results where the porosity at the surface ϵ_s was assumed to be greater than its initial value ϵ_0 . The calculation under this condition yields the decrease of ϵ in upper portion of sediment as shown in the figure.

Figure 13 compares the theory and experiments with respect to the sediment height. For the case of $E=125$ V/m, although the experimental value at the beginning of sedimentation agrees well with the calculated line under the condition $\epsilon_s=\epsilon_0$, it approaches the broken line of $\epsilon_s=0.955$. The surface layer may expand

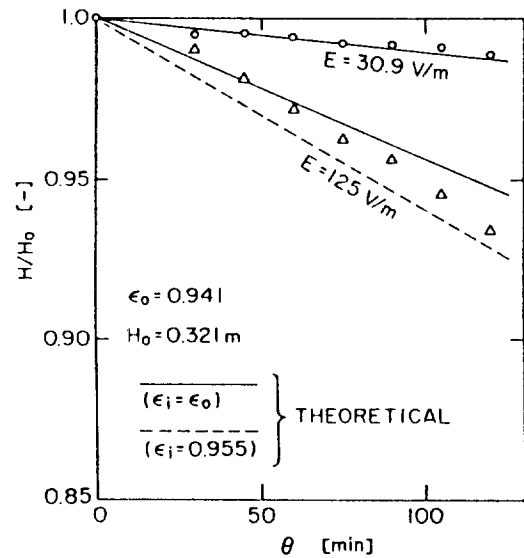


Fig. 13. Comparison of theoretical and experimental sediment height.

gradually from the initial structure to more loose structures.

CONCLUSIONS

The electroforced sedimentation process of a highly concentrated suspension has been investigated. Thickening due to consolidation proceeds from the bottom of sediment, but the compaction in the upper portion also occurs. The basic differential equation for this process is newly derived by use of Kobayashi's equations. It is also confirmed that the relation among hydraulic excess pressure, solid compressive pressure and gravity force in electroforced sedimentation is the same as in gravitational sedimentation due to consolidation. Based on the numerical calculation, the abnormal consolidation in the upper portion of sediment is induced by the expansion of surface layer due to electroosmotic flow.

NOMENCLATURE

- A : cross-sectional area of settling tube [m²]
- D : dielectric constant of fluid [F/m]
- D_e : equivalent diameter of flow path through sediment [m]
- E : intensity of electric field, that is, the applied voltage divided by the distance between electrodes [V/m]
- E' : intensity of electric field along the real flow path [V/m]
- e : local void ratio [-]
- F_D : viscous drag force acting on unit surface area of solid [N/m²]
- E_E : electrokinetic force acting on unit surface area of solid [N/m²]
- F_{GL} : gravitational force acting on unit volume of liquid [N/m³]
- F_{GS} : gravitational force acting on unit volume of solid [N/m³]
- F_s : compressive force propagated by solid structure [N]
- g : gravitational acceleration [m/s²]
- H : height of settling sediment [m]
- H₀ : initial height of sediment [m]
- i : electric current density [A/m²]
- P_L : local hydraulic pressure, which is the sum of p_L and static

pressure [Pa]

p_l : local hydraulic excess pressure [Pa]

p_s : local solid compressive pressure [Pa]

p_0 : p_c -value corresponding to initial porosity [Pa]

q : apparent velocity of liquid [m/s]

S_0 : volumetric specific surface [m²/m³]

v_0 : initial settling velocity [m/s]

x : distance measured from the bottom of sediment [m]

x' : spatial coordinate in the direction of real flow path [m]

α : specific hydrodynamic resistance [m/kg]

δ : thickness of electric double layer [m]

ε : local porosity [-]

ε_f : porosity at settling surface [-]

ε_0 : initial porosity of sediment [-]

ζ : zeta potential [V]

θ : settling time [s]

μ : liquid viscosity [Pa·s]

ρ : liquid density [kg/m³]

ρ_E : specific electric resistance [Ω m²/m]

ρ_s : true density of solid [kg/m³]

σ_s : effective charge on solid surface per unit volume of solid [C/m³]

ω : variable for representing an arbitrary position in the sediment, i.e. volume of solids per unit cross-sectional area measured from the bottom of sediment; $\omega = \int_0^x (1 - \omega) dx$ [m³/m²]

ω_0 : total volume of solid per unit cross-sectional area [m³/m²]

REFERENCES

- Iwata, M., Igami, H., Murase, T. and Yoshida, H., "Analysis of Electroosmotic Dewatering", *J. Chem. Eng. Japan*, **24**, 45 (1991).
- Kobayashi, K., Hakoda, M., Hosoda, Y., Iwata, M. and Yukawa, H., "Electroosmotic Flow through Particle Beds and Electroosmotic Pressure Distribution", *J. Chem. Eng. Japan*, **12**, 492 (1979).
- Kozicki, W., Chow, C. H. and Tiu, C., "Non-Newtonian Flow in Ducts of Arbitrary Cross-sectional Shape", *Chem. Eng. Sci.*, **21**, 665 (1966).
- Kozicki, W., Hsu, C. J. and Tiu, C., "Non-Newtonian Flow through Packed Beds and Porous Media", *Chem. Eng. Sci.*, **22**, 487 (1967).
- Shirato, M., Murase, T., Kato, H. and Fukaya, S., "Studies on Expression of Slurries under Constant Pressure", *Kagaku Kagaku*, **31**, 1125 (1967).
- Shirato, M., Kato, H., Kobayashi, K. and Sakazaki, H., "Analysis of Settling of Thick Slurries Due to Consolidation", *J. Chem. Eng. Japan*, **3**, 98 (1970).
- Shirato, M., Aragaki, T., Manabe, A. and Takeuchi, N., "Electroforced Sedimentation of Thick Clay Suspensions in Consolidation Region", *AIChE J.*, **25**, 855 (1979).